RESULT
Enhancing REServoirs in Urban deveLopmenT: smart wells and reservoir development, Geothermica Project Number 200317

RESULT-D5.2:
Optimised well concept for Dublin area

Responsible author:	Negar Khoshnevis Gargar (TNO) Slawomir Szklarz (TNO) Hans Veldkamp (TNO) Eduardo Barros (TNO) Jan Diederik van Wees (TNO)
Responsible WP-leader:	James McAteer (GDG)
Contributions by:	Jens Wollenweber (TNO)

Executive summary

This report presents results of the application of the well trajectory optimisation workflows to the Dublin case study. In particular, we focus on the application of robust optimisation under prior uncertainty, following the same approach recently presented in previous reports of the RESULT project (more focused on optimisation of cases in sedimentary systems). Based on the available information about the geological setting at the Dublin location, an ensemble of (dynamic) reservoir flow models was generated to represent the underlying geological uncertainty associated with the characterisation of the properties of the target reservoir formation, including uncertainty on the position and properties of high-permeability fault zones. Optimisation experiments were performed to search for the best location and shape of wells in a doublet configuration. Optimal solution found resulted in higher NPV than the initial solution. The obtained results show the adopted optimisation approach to be robust for handling structural uncertainty in the form of varying fault positions and model grids across the ensemble of model realisations. The optimal solution also provides insight into the most favourable relative placement of producer and injector wells of the doublet to be drilled along the fault zone. Despite the successful application of optimisation leading to techno-economic improvements, the relatively poor reservoir properties, low formation temperatures and large uncertainties result in a negative business case under the considered economic assumptions, indicating low potential for geothermal developments in the area and pointing to the need for additional information gathering activities in the area to allow more refined feasibility studies.

Table of Contents

1 Introduction

This report presents results of the application of the well trajectory optimisation workflows investigated in the RESULT project to the Dublin case study. In particular, we focus on the application of robust optimisation under prior uncertainty, following the same approach recently presented in RESULT reports D2.3, D3.1, D3.2 and D4.2 (focused on sedimentary systems). Based on the available information about the geological setting at the Dublin location, an ensemble of (dynamic) reservoir flow models was generated to represent the underlying geological uncertainty associated with the characterisation of the properties of the target reservoir formation, including uncertainty on the position and properties of high-permeability fault zones. Optimisation experiments were performed to search for the best location and shape of wells in a doublet configuration.

The report is structured as follows. First, the Dublin case study is introduced in Section 2, with a description of the target area (Figure 1), the information used to build static and dynamic simulation models (incl. geological uncertainties) and the economic assumptions guiding the optimization study. Next, in Sections 3 and 4 the optimisation study is presented, including a brief recap of the EVEReST framework used and the results of the performed optimisation experiments. Finally, the report is concluded with a summary of main findings obtained from optimisation results and insights to Dublin area.

2 Dublin case study

2.1 Dublin static model

A static model was built on the basis of a Petrel project originating from GSI and including updated fault location data including by iCRAG, namely the inclusion of the proposed Howth fault extension. This static model contains various gridded surfaces and faults. Properties were estimated in consultation with GDG.

Figure 1: Outline of the study area (in red). In grey the 3 main faults, including the Howth Fault (dashed) coming in from the Northeast over Sandymount.

2.1.1 Horizons

The stratigraphic succession under the Study Area includes the following layers (from top to bottom):

- Lucan Formation: The Lucan Formation comprises deep marine mudstones and siltstones which represent distal turbidites. The main lithologies are dark argillaceous limestones, shales and calcareous mudstones with some skeletal units and common chert and pyrite. The base depth is between 176 and 322 m.
- Tober Colleen Formation: The formation consists largely of cleaved mudrocks, usually with little carbonate, and rare boulder beds containing Tournaisian material. The mudrocks are slightly calcareous, becoming more so towards the top of the formation, and contain small micritic nodules and a number of allochthonous limestone blocks throughout the formation. The base depth is between 369 and 520 m.
- Waulsortian Formation: comprises massive, un-stratified limestone deposited in a shallow marine depositional environment. It is characterised by massive heterogeneous micrite with conspicuous sparry masses, stromatactis cavities and a fossil assemblage including bryozoans, corals and shells. The heterogenous micrite is thought to have formed from several generations of carbonate mud. The Waulsortian is susceptible to dolomitisation, most notably in proximity to faults, such as on the Howth peninsula. Karstification is common. The base depth is between 417 and 693 m.
- Ballysteen Formation, also known as Malahide formation or Boston Hill formation in County Kildare. It is characterised by the presence of a lower cyclic member and an upper laminated, cross-bedded grainstone interval, passing up near the top into nodular fine grained bioclastic limestone with thin shale interbeds. The base of the formation begins with up to 40 m of basal micrites and oncolites. Above are interbedded argillaceous biomicrites, biomicrites and biosparites with thicknesses of over 150 m. The top of the formation is dominated by calcareous muds and shales. Within the formation there are numerous faults along which dolomitisation is prevalent. These faults also act as conduits for mineralising fluids that have led to sphalerite, galena and chalcopyrite being common place. The base depth is between 535 and 1036 m.

Initially, Calp Lucan was identified as target aquifer, but below the study area it is present at very shallow depth. Therefore deeper strata were chosen as target, for instance the Waulsortian and Ballysteen formations.

2.1.2 Faults

Three faults were mapped in the study area through the GeoUrban project (
Figure 1). The main one is the Howth Fault. It was mapped in Dublin Bay, towards Sandymount, but it may well continue under Dublin towards the south-west (see below). It is considered an exploration target. The other two faults are located near the southern border of the area.

The width of the Howth fault zone or the fault zone permeability are unknown. However, it has a throw of over 300 m at the Howth peninsula which borders the northern Dublin Bay just northeast of Figure 1. High flow rates have been encountered in the onshore boreholes (near the Dublin port – in the northeast of the study area), which are likely to be associated with the Howth fault extending down southwest. Dolomitisation is pervasive in each borehole, with the intensity of fracturing increasing towards the west in the onshore boreholes BHO2 and BHO1. This suggests the presence of a substantial faulting in the area, possibly related to the continuation of the Howth Fault to the southwest. Boreholes M28 and M29 have also shown high levels of fracturing and dolomitisation suggesting these are also possible fault splays from the Howth Fault.

2.1.3 Properties

Exact porosity values for the formations are not available. For the model it was decided to rely on porosity values of analogous formations based on literature. When the rocks are not faulted or karstified, a porosity of about 5% and a permeability of about 2 mD is reasonable, although higher

GEOTHERMICA   RESULT

Optimised well concept for Dublin area

Doc.nr: RESULT-D5.2
Version: 2023.11.08
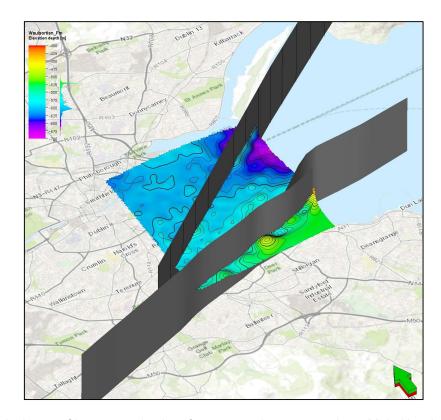Classification: public
Page: 6 of 15

permeability values may exist for deeper strata owing to fractures and dilation zones (e.g., Vozar et al. 2020).

The nearby deep borehole is at Newcastle, which is approx. 16km west of the study areaalong the Blackrock-Newcastle Fault (BNF), to which geothermal potential is attributed by Licciardi et al. (2017). Vozar et al. (2020) and Licciardi et al. (2017) mention secondary porosity and dilation zones at depths, which could be the case near Dublinas well. A major fault was encountered at a depth of 1,337 m dipping SE. Although no structural data are available below this depth, this fault is interpreted as a splay or a secondary fault of the BNF that contributes to create high secondary porosity at the base of the sedimentary sequence. Strongly fractured rocks with high secondary porosity have been found at the base of the borehole NGE1, and have been related to the presence of the BNF.

The highest fracture density (in depths of 1.015–1.075 km) and highest fluids inflow (in depths of 1.325–1.345 km) have been recorded in the borehole at Newcastle. Vozar et al. (2020) divided the Newcastle subsurface into two layered zones. The first zone, up to 1–2 km deep, is dominated by NE–SW oriented conductors that can be spatially connected with shallow faults probably filled with saline waters. The deeper conductive layers are interpreted as water- or geothermal fluid- bearing rocks, and the porosity and permeability estimations from the lithological borehole logs indicate the geothermal potential of the bedrock. The BNF is visible in their models as a conductive feature in the second zone and is interpreted to be a highly fractured fault system infilled by saline waters.

2.1.4 Model setup

The model was set up as a rectangle around the UCD, 6 km wide (EW) and 6.5 km long (NS) (Figure 1, Figure 2). The model contains the base Calp Lucan, Tobercullen, Waulsortian and Ballysteen – Boston Hill – Malahide horizons. The approximate increments of the Petrel pillar grid were 54 m X_{inc} and 66 m Y_{inc}, yielding 177 × 153 cells, and 30 layers. The Howth Fault was extended to the southwestern border of the model.

Figure 2: Geological area of interest and subsurface uncertainty assumptions. Main Howth Fault coming in from the North-East.
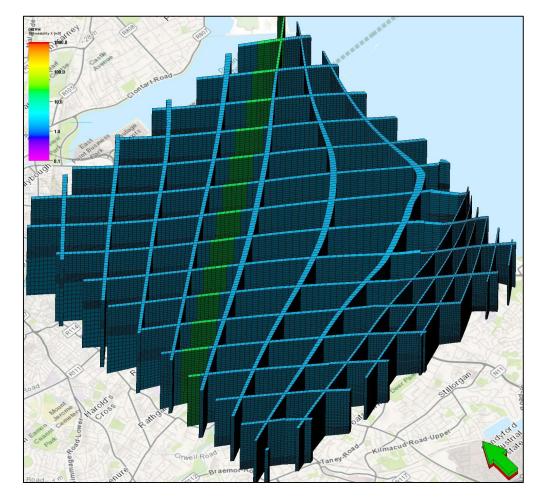
Because of the uncertainty regarding the reservoir properties and the exact location of the Howth Fault under Dublin, an uncertainty workflow was set up in which the properties shown in Table 1 were varied. The location and azimuth of the Howth Fault were varied, the azimuth with +/- 0.0-2.5° from the main bearing of 53 °N, and the location +/- 0-500 meter in the direction perpendicular to the bearing (uniform distribution). 10 fault realisations were generated, from which 10 pillar grids were built.

For each of the 10 pillar grids (see example in Figure 3), the properties fault damage zone width, fault damage zone porosity and permeability, matrix porosity and permeability, temperature gradient and surface temperature were varied, all drawing from uniform distributions. Because little data exist regarding the properties, the chosen ranges are wide and possibly can be regarded as optimistic, especially the potential fault zone width (cf. Childs et al. 2009 for a fault throw of 300 m).

Table 1: Uncertainty properties for the static model.

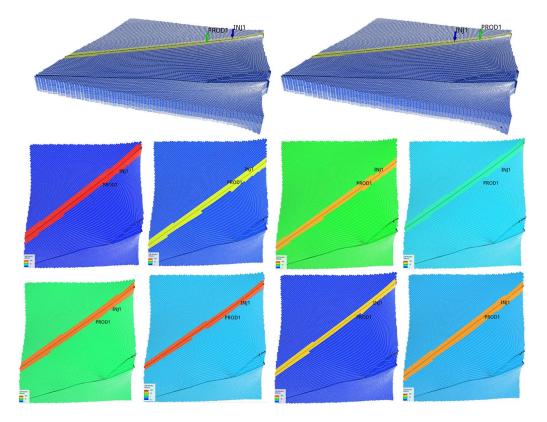|	min	max	unit
Fault location	-500	500	m
Fault zone width	150	300	m
Fault zone permeability	2	200[1]	mD
Matrix permeability	0.5	2	mD
Fault zone porosity	0.02	0.20	-
Matrix porosity	0.01	0.05	-
Temperature gradient	0.032	0.035	°C/m
Surface temperature	7	9	°C

Figure 3: Oblique view of one of the pillar grids showing the fault damage zone width and the permeability contrast between damage zone and matrix.

2.2 Dublin dynamic model

Geostatistical model realisations have been generated using the Petrel project created by TNO. Ensemble of 10 structural realisations of different fault location and width model has been created; each having 10 different static properties (i.e., porosity, NTG and permeability fields) to reflect the inherent geological uncertainties. The number of grid cells which varies slightly per model realisation depending on the fault location and width are 177 × 153 × 30, 176 × 153 × 30, 176 × 151 × 30 and 178 × 152 × 30, overall covering an area of approximately of 6 km x 6.5 km at an average depth of 200 m to 1000 m. Figure 4 shows several of model realisations randomly selected from the ensemble of 100 realisations.

Using the prepared static model, a dynamic reservoir simulation model was created. This was achieved by incorporating essential thermodynamic properties for the reservoir's fluids, accounting for interactions between the rock and fluids, considering the compressibility and thermal characteristics of the rock, and initialising the reservoir's pressure and temperature conditions. Furthermore, a geothermal doublet was integrated into the model by locating a vertical production well and an injection well along the fault. These wells (different well configurations) provided the initial starting points for the optimisation exercises that will be elaborated upon later. The water injection rate has been dynamically allocated, ensuring that the produced volumes are reinjected. This allocation is achieved through a combination of group control keywords managed by the reservoir flow simulator. The temperature of re-injected water is set to 25 °C.

Figure 4: Dublin reservoir model with two different well type configurations (top figure) and different grid structure (fault positions) and permeability fields for eight model realisations (bottom figure).

2.3 Economic parameters

The calculation for the business case is made in line with Dutch geothermal sector. As there is currently no support scheme for geothermal developments in Ireland, we used a feed in price in line with the Dutch feed in scheme (called SDE) for 15 years. For most geothermal projects in the Netherlands an economic life-time of 30 years is aimed for. The Net Present Value (NPV) of this concept is determined by factoring in depreciation and the discount rate. Income is computed based on the heat generated, basic heat price and for the first 15 years replaced by the feed in price. It's worth noting that the heat itself holds intrinsic value, though this value can significantly differ from one project to another.

The objective of this study is to optimise the economic viability of heat production in a geothermal project over a 30-year production life-cycle. To achieve this, a conventional Net Present Value (NPV) calculation method, as outlined in prior work (Van Wees et al. 2012), has been employed. This NPV calculation incorporates the time-value considerations associated with heat production and its associated costs.

$$J_{\text{NPV}}(\mathbf{u}) = \sum_{k=1}^{N_{\text{t}}} \frac{\left(r_h \cdot e_{\text{prod},k}(\mathbf{u}) - r_p \cdot \left(e_{\text{pump},k}^{\text{prod}}(\mathbf{u}) + e_{\text{pump},k}^{\text{inj}}(\mathbf{u})\right) - c_k(\mathbf{u})\right)}{(1+b)^{t_k/\tau}}, \tag{1}$$

In this equation, $\mathbf{u}$ represents the control vector, $e_{\text{prod},k}$ signifies the heat production during the kth simulation time interval, $e_{\text{pump},k}$ denotes the energy consumed by the necessary pumps, c_k encompasses the associated costs (comprising CAPEX and OPEX), r_h stands for the heat price [€/kWh] (inclusive of the SDE+ subsidy over a 15-year duration), r_p represents the electricity cost [€/kWh] for operational purposes, b is the discounting factor, t_k signifies the time at the kth simulation time-step, τ serves as the reference time for discounting cashflows, and N_{t} corresponds to the total number of simulation time-steps.

The computed energy output at each time-step, denoted as $e_{\mathrm{prod},k}$ [W=J/s], is determined as follows:

$$e_{prod,k} = q_k \rho_w c_w \Delta T_k \, , \tag{2}$$

where q_k [m³/s] represents the volumetric production rate and ΔT_k [K] indicates the temperature difference between injection and production at each simulation time-step k. ρ_w [kg/m³] stands for water density and c_w [J/kg·K] represents water's specific heat capacity.

The pumping costs are computed for both injection and production wells, which are influenced by the energy needed for pumping. In the case of producers, this calculation is dependent on the pump's efficiency (ε), the production rates q_k [m³/s], and the pressure difference $\Delta P_{prod,k}$ [bar] imposed by electrical submersible pumps (ESPs) to lift the produced fluids to the surface facilities.

$$e_{pump,k}^{prod} = \frac{q_k \Delta P_{prod,k}}{\varepsilon} \, . \tag{3}$$

For the injectors, booster pump is employed at the surface, positioned downstream of the heat exchanger, to facilitate the injection of cold water into the wells. The energy expended in operating this booster pump is computed as follows:

$$e_{pump,k}^{inj} = \frac{q_k \Delta P_{inj,k}}{\varepsilon} \, . \tag{4}$$

The CAPEX costs cover all expenses related to surface facilities, including heat exchangers, booster pumps, and, if needed, separators. These costs are assumed to be invested in the initial year of project development. In this study, drilling costs are determined based on the length of each well drilled. Additionally, ESPs entail their own associated costs as they are periodically replaced in the production wells. The OPEX costs for both producers and injectors are calculated separately. The specific economic parameters used for the NPV calculation are detailed in Table 2.

Table 2: The economic assumptions used in the optimisation experiments.

Variable	Value	Variable	Value
wellcost_base	250e3 EUR	loan_nyear	15 years
wellcost_linear	1000 EUR/km	loan_rate	0.05 loan rate
pump_efficiency	0.65	discount_rate	0.15
pump_cost	0.5e6 EUR	inflation_rate	0.02
pump_life	10 years	tax_rate	0.25
CAPEX_base	3e6 EUR	tax_depreciation_nyear	15
CAPEX_variable	300 EUR/kWth	heat_price	5 EURct/kWh
OPEX_base	10 000 EUR/year	heat_price_feedin	5 EURct/kWh (for subsidy years)
OPEX_variable	0 EUR/kWth	electricity_price	5 EURct/kWh
		injection_temperature	25 C

3 Optimisation of well design

In this section we present the results of the robust optimisation performed to optimise the well design (i.e., well trajectory and well locations) in the Dublin case study under prior geological uncertainties. The theoretical background of robust optimisation was described in more details in report RESULT-D2.3 prepared by TNO in earlier tasks of the RESULT project. The general idea behind robust optimisation is to formulate an optimisation procedure aiming at finding a single solution which is optimal over an ensemble of model realisations. This is typically achieved by considering an objective function calculated as the mean (or average) of the objective function values computed individually for each model realisation, while all realisations are assumed to be equiprobable. The robust solution is often not the best performing one for each model realisation, but it is the best performing one on average. The rationale is that a solution obtained through such procedure is robust against the uncertainty (or variability) of models considered. As presented in report RESULT-D2.3, TNO's in-house optimisation technology (EVEReST), built upon the recently developed stochastic gradient-based optimisation technique StoSAG (Fonseca et al., 2017), allows to perform robust optimisation in a computationally efficient manner – i.e. with much fewer numerical simulations required when compared to alternative techniques. Figure 5 depicts schematically the robust optimisation process.
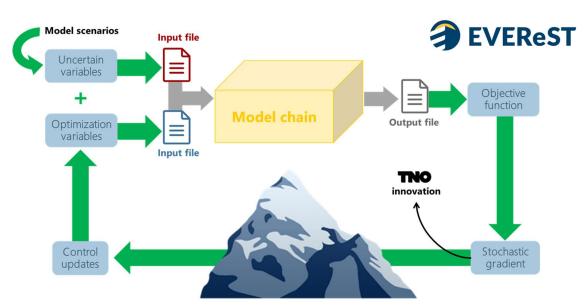

Figure 5: Schematic representation of the robust optimisation process in terms of input and output.

In this study, we refer to optimisation under prior geological uncertainties meaning that the model realisations considered within the optimisation characterise the initial state of uncertainty – i.e. the model realisations reflect the knowledge of the local geology available at the design phase, before drilling any of the planned wells. Thus, here the prior ensemble of model realisations refers to the collection of models described in Section 1.
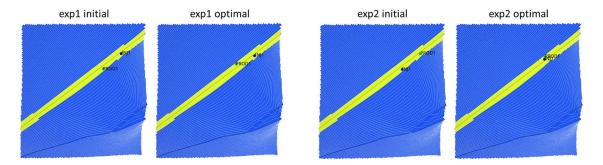
The optimisation variables in this robust optimisation experiment are the coordinates of the guide points defining the well path geometry, following the same approach described in reports RESULT-D3.1 and RESULT-D3.2 (and introduced in Barros et al., 2020) where well trajectory optimisation was applied to a simple synthetic benchmark model representative of sedimentary geothermal reservoirs in the Netherlands. The parametrisation of well trajectories through a few guide points allows the optimiser to explore a variety of well design configurations, ranging from vertical to deviated and horizontal wells.
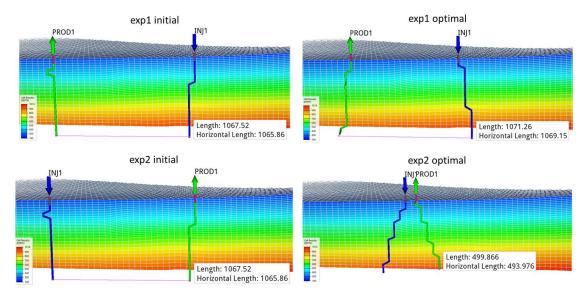
4 Results

We conducted an optimisation process to determine the trajectories and placements of a doublet system. This optimisation aimed to discover a solution that, on average across 100 different model realizations accounting for geological and structural uncertainties, yields the highest NPV. Due to the presence of more favourable flow properties near the fault, we created initial guess by placing a doublet approximately along the fault zone. We carried out two distinct optimization experiments, each considering different initial well placement for the producer and injector along the fault zone:

▪ Experiment 1: initial well placement with producer at west of injector
▪ Experiment 2: initial well placement with producer at east of injector

Figure 6: Well locations for initial and optimal solutions shown for 1st geological (and structural) realization for both experiments.
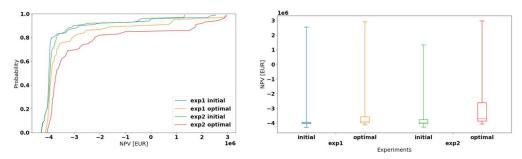
Figure 6 illustrates both the initial and optimal solutions regarding the placement of well locations. In optimal solutions of each experiment the well distance is shorter than in the initial guess. However, in the Experiment 2 the optimal well locations resulted in significantly shorter distance than in Experiment 1. At the same time, the Experiment 2 resulted in the highest average NPV, see Figure 8. As a result of the reservoir's low permeability, there is no observable occurrence of cold water breakthrough in the model, as evidenced by the temperature profile depicted in Figure 9. Consequently, reducing the distance between the wells will not result in a decrease in heat production. From a cost perspective, it is more economical to position the wells closer together due to the reduced drilling distance from the surface drilling location.

Figure 7: Well trajectories for initial and optimal solutions shown in a cross section along the fault for 1st geological (and structural) realization for both experiments. Vertical scale 5:1.
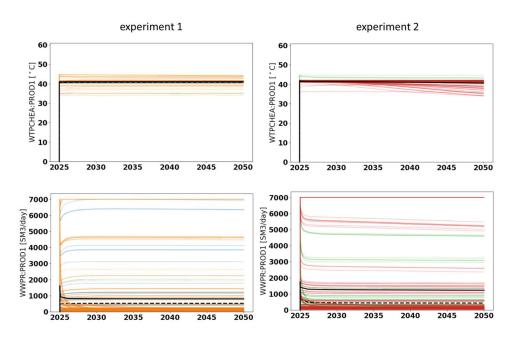
Even though the initial trajectory shape is vertical, the optimization has a freedom to change it as long as the drilling constraints (i.e. dogleg) are respected ensuring the drilling feasibility. In both optimisation experiments, both wells become slightly deviated with the stronger effect observed in Experiment 2. Because of the poor permeability characteristics found in both the matrix and the fault, the optimizer tries to enhance the contact of the wells with the reservoir in order to increase heat production. This is achieved by taking into account the drilling cost, which is contingent on the length of the well. In addition, the distance between the wells increases with the depth, see Figure 7.

Figure 8: Cumulative density functions (CDFs) of the objective function (NPV) for initial guess and optimal strategies for both experiments.

The objective function of the optimisation experiments was to find the optimal well trajectories and locations in terms of average NPV value across the model realizations. The distribution of NPV values (being optimized) for both initial and optimal scenarios can be seen in Figure 8.

Figure 9: Temperatures and production rates in the producers for initial and optimal well locations/trajectories for all experiments. Each coloured line represents one geological realisation. Dashed line shows average for the initial guess and solid line represents optimal solution.

In both optimisation experiments optimal solutions resulted in higher NPV than in the respective initial guesses (only well type differed between initial guesses). However, Experiment 2 resulted in significantly higher NPV on average than Experiment 1. The significant impact on the cost-effectiveness of the project has the combination of production temperature and production rates. The production temperature profiles in optimal solution of both experiments remain comparable, i.e.

no significant cold water breakthrough is observed in production wells. However, the average production rates are almost doubled in the Experiment 2, which positively influences NPV value.

5 Conclusions

To summarise the main findings obtained from this study, we can list:
- Optimal solutions resulted in higher NPV than in the respective initial guesses in both optimization experiments performed, confirming usefulness of optimization.
- Despite free to explore other configurations, optimiser confirms that most favourable placement of the doublet is within the fault zone.
- Adopted optimisation approach has shown to be robust to successfully handle structural uncertainty in the form of varying fault positions and model grids across the ensemble of model realisations.
- Drilling the producer to the east of the injector and reducing the spacing between wells by changing them into slight deviated wells (Experiment 2) resulted in best techno-economic performance.
- Relative poor reservoir properties and low formation temperatures result in a negative business case under considered economic assumptions, indicating low potential for geothermal developments even after optimisation.
- Due to lack of more detailed knowledge about the area, large conservative estimates of uncertainty were taken into account. Information gathering activities should be considered to improve knowledge of the area for future feasibility studies.
- Most room for improvement in optimisation seems to be associated with best performing model realizations, with some of them achieving a positive business case. The gains in NPV on average are more modest due to the many poorly performing realisations.

6 References

Barros, E.G.D., Chitu, A., and Leeuwenburgh, O. (2020). Ensemble-based well trajectory and drilling schedule optimization - Application to the Olympus benchmark model. *Computational Geosciences*, **24** (4), 2095-2109. https://doi.org/10.1007/s10596-020-09952-7.

Barros, E.G.D., Szklarz, S.P., and van Wees, J.D.A.M. (2021). RESULT-D2.3: Drill & Learn Approaches.

Barros, E.G.D., Szklarz, S.P., Khoshnevis Gargar, N., and van Wees, J.D.A.M. (2021). RESULT-D3.1: Optimization Model Framework.

Bruijnen, P. and Leewis, M. (2022). RESULT-D4.1: 3D Reservoir Characterization Model for Zwolle.

Childs, C., Manzocchi, T., Walsh, J.J., Bonson, C.G., Nicol, A., Schöpfer, M.P.J. (2009). A geometric model of fault zone and fault rock thickness variations. J. Struct. Geol., 31 (2009), pp. 117-127, https://doi.org/10.1016/j.jsg.2008.08.009

Fonseca, R.M., Chen B., Jansen, J.D., and Reynolds, A.C. (2017). A Stochastic Simplex Approximate Gradient (StoSAG) for optimization under uncertainty. *International Journal for Numerical Methods in Engineering*, **109** (13), 1756-1776. https://doi.org/10.1002/nme.5342.

Licciardi, A. and Agostinetti, N.P. (2017). Sedimentary basin exploration with receiver functions: Seismic structure and anisotropy of the Dublin Basin (Ireland). *Geophysics* 82 (4) 1-62. DOI: 10.1190/geo2016-0471.1

Van Wees, J.D., Kronimus, A., Van Putten, M., Pluymaekers, M., Mijnlieff, H., Van Hooff, Obdam, A., Kramers, L. (2012). Geothermal aquifer performance assessment for direct heat production. Methodology and application to Rotliegend aquifers. Netherlands Journal of Geosciences 91-4, 651-665. 54.

Vozar, J., Jones, A.G., Campanya, J., Yeomans, C., Muller, M.R. and Pasquali, R. (2020). A geothermal aquifer in the dilation zones on the southern margin of the Dublin Basin. *Geophysical Journal International*, **220**, 1717-1734. http://doi.org/10.1093/gji/ggz530.